Rock and Soil Mechanics

Volume 41 | Issue 12 Article 7

4-29-2021

Load test study of bearing characteristics of reinforced soil abutments

Xiao ZHANG
Department of Geotechnical Engineering, Tongji University, Shanghai 200092, China

Chao XU
Key Laboratory of Geotechnical and Underground Engineering of Ministry of Education, Tongji University, Shanghai 200092, China

Qiu-shen WANG
Department of Geotechnical Engineering, Tongji University, Shanghai 200092, China

Wei-cheng WU
Department of Geotechnical Engineering, Tongji University, Shanghai 200092, China

Custom Citation

ZHANG Xiao, XU Chao, WANG Qiu-shen , WU Wei-cheng, . Load test study of bearing characteristics of reinforced soil abutments[J]. Rock and Soil Mechanics, 2020, 41(12): 4027-4034.

Rock and Soil Mechanics 2020 41(12): 4027−4034 ISSN 1000−7598
https: //doi.org/10.16285/j.rsm.2020.5390 rocksoilmech.researchcommons.org/journal

Load test study of bearing characteristics of reinforced soil abutments

ZHANG Xiao[1], XU Chao[1, 2], WANG Qiu-shen[1], WU Wei-cheng[1]
1. Department of Geotechnical Engineering, Tongji University, Shanghai 200092, China
2. Key Laboratory of Geotechnical and Underground Engineering of Ministry of Education, Tongji University, Shanghai 200092, China

Abstract: As a bearing structure, the reinforced soil abutment has attracted much attention for its bearing capacity and its influencing factors. Taking the Bowman bridge as the engineering prototype, this paper studies the bearing capacity of the reinforced soil flexible abutment by the scale model test. In the experimental study, three groups of load tests of the reinforced soil flexible abutment were set up, which uses the geotextile as the reinforcement material. This paper mainly studies the influence of bridge base position on the bearing capacity of the abutment. Test results show that the setback is an important factor affecting the bearing capacity of the reinforced abutment, and that the bearing capacity increases with the setback, but the amount of increase is rapidly diminishing. The horizontal and vertical settlements at the top of the abutment decrease with the increase of the setback, and the decreasing trend shows convergence. With the increase of setback, the maximum strain of reinforcement decreases, and the overall stability of abutment is enhanced, showing better complex characteristics. In addition, the results of this experimental study also prove that the calculation method of bearing capacity of reinforced abutments in the current US regulations may be limited to specific packing and reinforcement arrangement. Therefore, it should be combined with actual conditions in engineering practice.

Keywords: geosynthetics; reinforced soil abutment; load-bearing characteristics; load test

1 Introduction

The geosynthetic reinforced soil-integrated bridge system (GRS-IBS) is composed of the geosynthetic reinforced soil abutment, the bridge structure and the connecting subgrade. The abutments on both sides are alternately filled using compacted filling and small spacing (less than or equal to 300 mm) reinforced materials, which is convenient and quick to construct, and has significant advantages over pile-supported abutments[1]. Overseas researchers performed long-term performance monitoring of the GRS-IBS during the normal service period[2−5]. They confirmed that the structure has good working performance under the influence of external environmental factors such as vehicle load, overload, and temperature. Through integrated design and construction, GRS-IBS can theoretically eliminate the differential settlement between the bridge and the subgrade of the approach road. Consequently, it can solve the problem of bumping at bridge head.

As a load-bearing structure, the load-bearing performance and influencing factors of reinforced soil abutments have attracted much attention . Hoffman et al.[6], Nicks et al.[7], Cai[8] and others found that the spacing and stiffness of the reinforcement are important influencing factors of the bearing capacity of the abutment through the study of miniature piers and scaled models. Xu et al.[9] pointed out that the spacing of vertical reinforcement has a more significant influence on the stability of abutment. Wang et al.[10] suggested the reasonable spacing of the GRS abutment to be 30−50 cm. Wu et al.[11], Xu et al.[12] and other researchers proposed calculation methods of the ultimate pressure of the GRS composite based on the quasi-cohesive reinforcement mechanism and the equivalent confining pressure incremental reinforcement principle, respectively.

As a bearing structure, the bearing capacity of the GRS abutment is also related to the distance between the bridge foundation and the abutment surface. Xiao et al.[13] carried out an experimental study on the influence of the bridge foundation and the horizontal clearance of the reinforced soil abutment slab on the bearing capacity of the abutment, and obtained the relationship between ultimate bearing capacity of the abutment and the horizontal clearance. Murad et al.[14] also found through numerical simulation that the horizontal clearance and foundation width have certain effects on the bearing capacity of the abutment, but these findings have not been verified by corresponding model tests.

Based on the existing research results, engineering experience of reinforced soil abutments and GRS-IBS, this study uses geotextiles as reinforcements, blocks as surface layers, and uses large-scale scaled model static load test to further study the bearing capacity and deformation characteristics of reinforced soil abutments and their changes with the position of the bridge bearing area.

For the convenience of the following description, the horizontal distance between the outer edge of the bridge

Received: 3 April 2020 Revised: 22 June 2020
This work was supported by the Key Research and Development Project for the Ministry of Science and Technology of China(2016YFE0105800).
First author: ZHANG Xiao, male, born in 1996, Master candidate, majors in geosynthetics reinforced soil structure. E-mail: 1830163@tongji.edu.cn

seat (or the top bearing area of the abutment) and the reinforced soil abutment deck is defined as the horizontal clear distance, which corresponds to the "setback" of the bridge foundation in the literature.

2 Model test

2.1 Test model and material

The model is based on the Bowman Bridge in Ohio, USA as the engineering prototype. The model test relies on the vehicle load simulation loading platform at the Key Laboratory of Road and Traffic Engineering of the Ministry of Education, School of Transportation Engineering, Tongji University. Limited by the size of the test site and actual loading conditions, the model is scaled as 1:3. The main geometric dimensions of the engineering prototype and model are shown in Table 1.

Table 1 Parameters for engineering prototype and test model

Type	Abutment height /m	Foundation height /m	Embankment high /m	Wall width /m	Wall base length /m	Wall top length /m	Bridge bearing area length *b* /m	Base length /m	Horizontal clearance /cm	Reinforcement spacing /cm
Engineering prototype	4.70	0.45	0.9	13.3	1.8	5.5	1.2	2.30	20	20
Indoor model	1.46	0.15	0.3	1.5(plane strain)	0.6	1.8	0.4	0.75	30 reference	14

The proposed model is a unilateral abutment as a GRS-IBS structure. As shown in Fig. 1, the model consists of five parts: GRS abutment, reinforced foundation, foundation soil and backfill, the integrated approach, the bridge structure. The model has a total length of 3.4 m, a total height of 1.91 m, and a total width of 1.5 m. The total height *H* of the GRS abutment is 1.46 m. The slope of the abutment fill is consistent with the prototype, both are 1:1. The width of the bridge bearing area is 0.4 m, and the size of the integrated approach changes with the horizontal clearance.

The reinforcement spacing is set to 14 cm (twice the layer spacing), which reduces the ultimate bearing capacity of the abutment model under the principle of closely spaced geosynthetic reinforcement, so that the abutment failure can be achieved more easily. According to the design requirements of the current American standard[15], the reinforcement length of the densely reinforced area under the abutment base is not less than twice the sum of the horizontal clear distance and the bridge bearing area, which is set to 1.27 m.

The variable involved in this model test is the horizontal clear distance. The L-shaped steel plate is used to replace the bridge structure to be in contact with the bridge abutment. The steel rail is welded to meet its rigidity requirements. Its size is 0.4 m×1.5 m, and the bridge structure weight is added to be part of the abutment loading. The evenly distributed precast concrete test blocks are used to simulate the filling of the integrated approach area. The model test meets the plane strain condition. One side of the model is set as a steel plate wall, and the other side is set as a plexiglass baffle. Cross marks in corresponding colors are pasted on the inside and outside of the plexiglass plate to facilitate the observation of the overall deformation trend of the abutment.

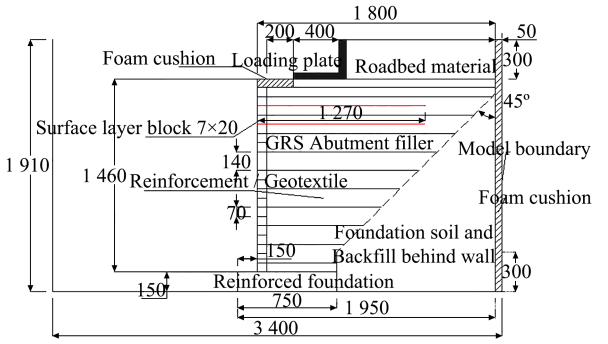

(a) Model profile

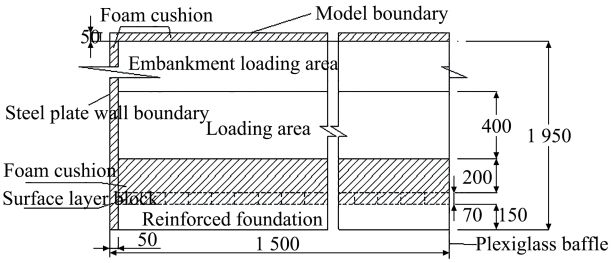

(b) Planar graph

Fig. 1 Configuration of test model(unit: mm)

In the experiment, self-made cement mortar blocks were used as the surface layer of the bridge abutment, and the scaled size was 130 mm×70 mm×70 mm. The surface layer blocks were stacked in layers and staggered joints, and the reinforcement materials were sandwiched between the two layers of blocks, connected by friction.

In the experiment, PP bidirectional geotextile was selected as the reinforcement material. According to the dimensional analysis, the tensile strength corresponding to 10% strain of the reinforcement should be 8 kN/m, and the tensile test result of the reinforcement (see Fig. 2) shows that the test value corresponding to 10% strain is 7.53 kN/m. Values from both tests are similar and they practically meet the design requirements.

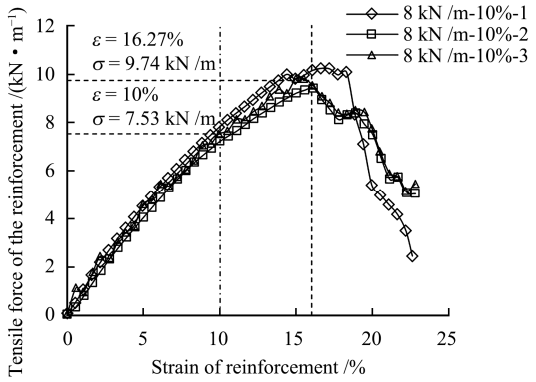

Fig. 2 Tensile tests of reinforcement

The particle size of the engineering prototype fill ranges from 0.3 to 12.7 mm. According to the scale of the model, quartz sand with a particle size ranging from 0.1 to 4.2 mm is selected for the experiment. The modified analog method is used to determine the gradation of the fill, and the particle size is specified based on the prototype. The specified particle size of the model and the corresponding sieving rate are calculated, and the gradation curve of the selected fill in the experiment is shown in Fig. 3. The maximum dry density of the fill is 1.86 g/cm^3. Through the GDS stress path triaxial test, when the degree of compaction is 95%, the internal friction angle φ of the fill is about 48º, and the cohesion c is 0 kPa.

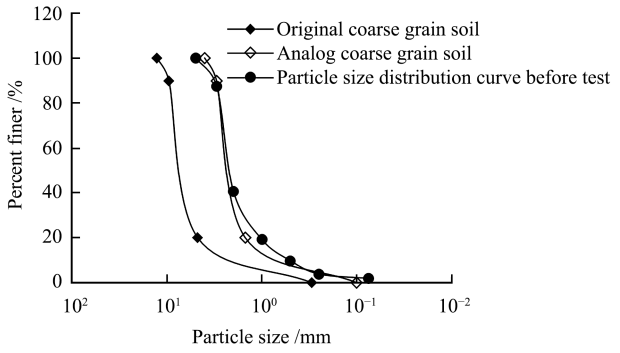

Fig. 3 Grain size distribution of sands used in tests

2.2 Test scheme and test method

According to the characteristics of the prototype and actual test conditions, a total of 3 sets of model tests were designed. The test scheme is shown in Table 2.

Table 2 Model test scheme

Test number	Horizontal clearance /cm	Spacing of reinforcement /cm
T1	20	
T2	30 reference	14
T3	40	

According to the evaluation in the U.S. standard[15], the ultimate bearing capacity of GRS abutment is 48 kPa, which was converted to an upper load of about 30 kN. Based on the capacity of the loading equipment, it was planned to determine the maximum loading value of the model as 3 times the ultimate bearing capacity. The static load mode of the hydraulic pulsation fatigue testing machine was used. The shallow foundation plate load method was adopted as a reference. The load was gradually loaded from scratch, and the graded load is 10 kN in each step. The load test is terminated when there was obvious signs of failure in the whole sample and when the overall settlement of the model reached 5% of the abutment height (i.e. 7.5 cm), or when the maximum horizontal displacement of the surface layer reached 10% of the abutment height (i.e. 15 cm).

2.3 Monitoring scheme

The monitoring parameters in the test includes the settlement at the top of the abutment, the horizontal displacement of the surface, the horizontal and vertical applied stress in the GRS abutment, the strain of the reinforcement, and the overall deformation trend of the abutment is observed and recorded. The layout of monitoring instrumentation is shown in Fig. 4.

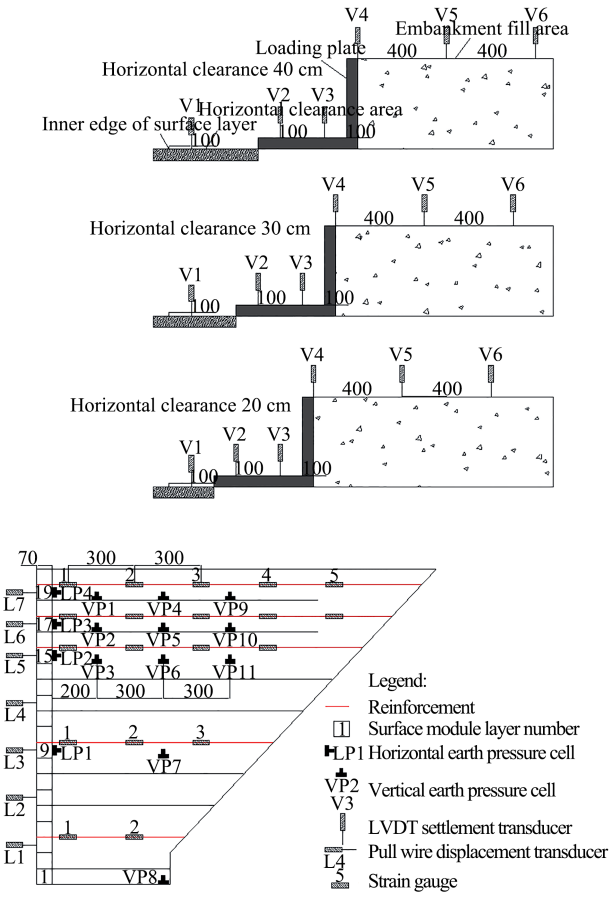

Fig. 4 Monitoring scheme (unit: mm)

2.4 Model construction

Following the procedures of reinforced foundation

construction−abutment filling−bearing area treatment−loading slab placement, the abutment is constructed. The completed abutment model is shown in Fig. 5. Before the abutment is filled, the sidewall resistance reduction treatment is carried out by pasting a PTFE film and then applying lubricant. During the construction process, the volume−mass method was used to control the compaction degree of fills in layers to be above 95%. The layer thickness is 7 cm, and the filling was divided into 21 layers. During the stacking process of the surface layer, a cross level gauge is used to check the level, and the surface layer baffle is set to prevent the surface layer from tilting. The contact area of the surface layer and the outer wall side wall is filled with foam sheets of appropriate size to prevent sand leakage and to reduce side resistance.

Fig. 5 Test model

3 Test results and analysis

The collected data is marked and calibrated in different directions according to engineering practice. For the displacement of the surface layer, the direction towards the free surface is positive. For the settlement of the top of the abutment, the downward is positive. For the additional stress in the abutment, the compressive stress is positive. The strain of the reinforcement is positive when it is subject to tensile stress.

3.1 Description of observations in the test

The threshold of the loading device of the test equipment is 100 kN, so the maximum load of the test can only reach 100 kN. Under this load, the three groups of abutment models did not undergo significant deformation and failure. Only a small degree of outturn was observed in the middle and upper parts of the surface layer, and local fillers were squeezed into the surface layer and side walls. A small amount of settlement was observed at the top of the abutment. Reinforcing bars changed from horizontal to be curved, and the cross-mark points on the inner and outer sides of the organic glass baffle were obviously misaligned, as shown in Fig. 6. The model as a whole had no signs of damage such as sudden changes in surface displacement, significant settlement at the top, or fracture of the reinforcement. This test result shows that the actual ultimate bearing capacity of the abutment should be much greater than the value calculated by the formula. Xu et al.[12] pointed out that the reason is that the formula only verifies the composite structure of large-particle fillers (filler's maximum particle size greater than 10 mm). However, it does not consider that the small-particle fillers (filler's maximum particle size less than 5 mm) has a weakening effect on the impact factor W. At the same time, as a load-bearing structure, the ultimate bearing capacity of the reinforced abutment is bound to be affected by factors such as the horizontal clearance, the width of the beam seat, and the size of the reinforced foundation. The test results in this paper prove that the formula without considering the horizontal clearance has a large prediction error for the ultimate bearing capacity

(a) Side wall of facing layer inclines outwards

(b) Filling is squeezed into side wall block

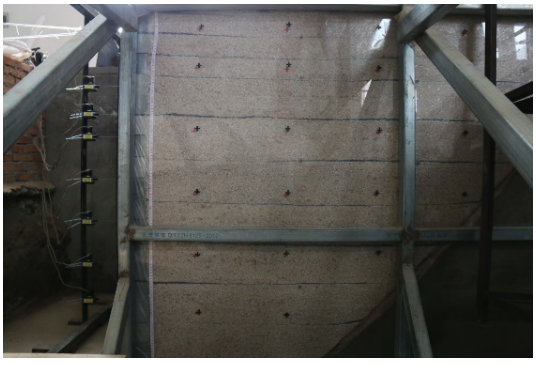

(c) Partial deflection of Geotextiles

Fig. 6 Local damage of abutment structure after test

of reinforced abutments. Therefore, the ultimate bearing capacity formula given by the American Code[15] may only be applicable to specific fillers, reinforcements and a specific layout of reinforcements. Therefore, in actual engineering applications, not only the impact of the horizontal clearance on the bearing capacity should be considered, but also the actual engineering practice should be combined when using the bearing capacity calculation formula in the American standard.

The monitored physical quantities vary with the change of the horizontal clearance, and the degree of outward inclination of the surface layer does not show a significant correlation with the change of the horizontal clearance. The horizontal displacement and top settlement of the surface layer decrease with the increase of the horizontal clearance. The degree of deflection of the reinforcement in the fill decreases with the increase of the horizontal clearance, but there is no obvious cracking phenomenon.

3.2 Load−settlement curve

Figure 7 shows three sets of model test load−settlement (*p*-*s*) curves. In general, each set of curves is approximately linear, indicating that the abutment model has not reached the ultimate failure state, and as the horizontal clearance increases, the abutment settlement decreases. When the horizontal clear distance decreases from 30 cm to 20 cm, the settlement increases significantly; while the horizontal clearance increases from 30 cm to 40 cm, the two *p*-*s* curves are very similar to each other, indicating that when the horizontal clearance meets certain requirements, increasing the horizontal clearance afterwards has little effect on the overall bearing capacity of the abutment. In the model T1 test, there was a sudden change in settlement, and then the settlement increased linearly with the load. The reason might be that the loading device was abnormal when a load of 50 kN was applied.

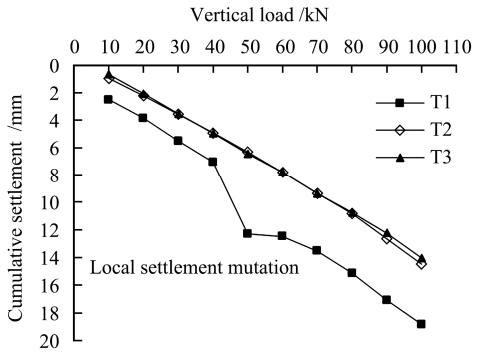

Fig. 7 *p*-*s* curves of load test

3.3 Settlement at the top of abutment

As shown in Fig. 8, the cumulative settlement at the top of each model abutment under a load of 100 kN follows the same distribution law. The settlement of the bridge bearing area is large and much larger than that of other areas. The settlement at the top of the model is much smaller than the settlement (5%*H*) under its ultimate bearing state. This indicates that the abutment model is still in normal service. Comparing T1, T2, and T3, it can be found that with the gradual increase of the horizontal clearance, the settlement of the bridge bearing area first decreases significantly, and then changes little. This result is consistent with the aforementioned load−settlement curve. The settlement on the side close to the surface layer decreases slightly with the increase of the horizontal clearance, while the settlement in the integrated approach area increases slightly. The settlement on the top of the abutment is gradually dispersed from the bearing area to both sides, and the abutment model shows an improved ability in deformation coordination as a feature of complex materials.

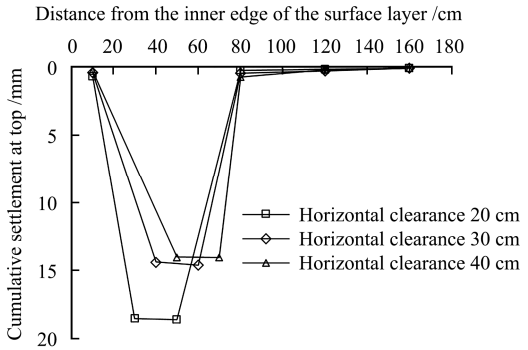

Fig. 8 Settlement distribution of abutment top under 100 kN load

3.4 Horizontal displacement of surface layer

Figure 9 shows the distribution of the displacement along the wall height of each abutment under a load of 100 kN. It can be seen that with the gradual increase of the horizontal clearance, the horizontal displacement of the surface layer continues to decrease and tends to be evenly distributed along the wall height. The maximum value of the horizontal displacement of the surface layer of each bridge abutment is achieved at the location of about 1/3*H* from the top of the abutment.

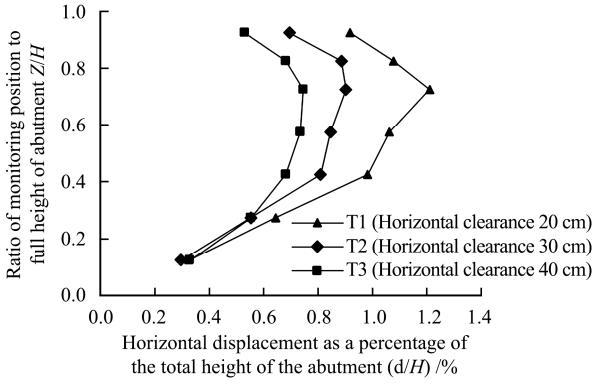

Fig. 9 Surface displacement distribution under a 100 kN load

From the analysis of the top settlement and lateral displacement of the reinforced soil abutment under the vertical load as shown in Fig. 7 to Fig. 9, the bearing capacity of the reinforced soil abutment increases with the increase of the horizontal clearance. However, from the results of the three sets of model tests presented in this paper, the increase in bearing capacity was significantly reduced when the horizontal clearance increased from 20 cm to 30 cm, and from 30 cm to 40 cm. This shows that reinforced soil abutments should have a certain horizontal clearance, but an excessively large horizontal clearance is of little significance and it also increases length of the bridge structure, which is unreasonable.

3.5 Vertical additional stress

Figure 10 shows the distribution of the vertical additional stress inside the abutment model under a load of 100 kN. Overall, the horizontal distribution of vertical earth pressure inside the reinforced abutment is more consistent with the theoretical solution obtained by the corner point method under rectangular uniformly distributed load. Both show that the earth pressure in the middle part is larger and the earth pressure near the two sides is smaller. The measured value of earth pressure under the loading plate is obviously higher than the theoretical value, but the opposite is true when it is far from the bearing area, indicating that a certain degree of stress concentration will occur under the loading position. This result confirms the rationality of reducing the spacing of the reinforced layers within a certain depth below the bearing area. Since the size ratio of the bearing area to the top of the abutment model does not satisfy the assumption of uniform load in a semi-infinite space, and the reinforced soil composite is an anisotropic medium, the measured value and the theoretical solution are somewhat different. In addition, in the three groups of model tests, with the change of the horizontal clearance, the earth pressure distribution law is not the same, and the degree of agreement between the measured value and the theoretical solution is also different, indicating that the horizontal clearance has a certain influence on the earth pressure distribution. The mechanism needs to be further explored.

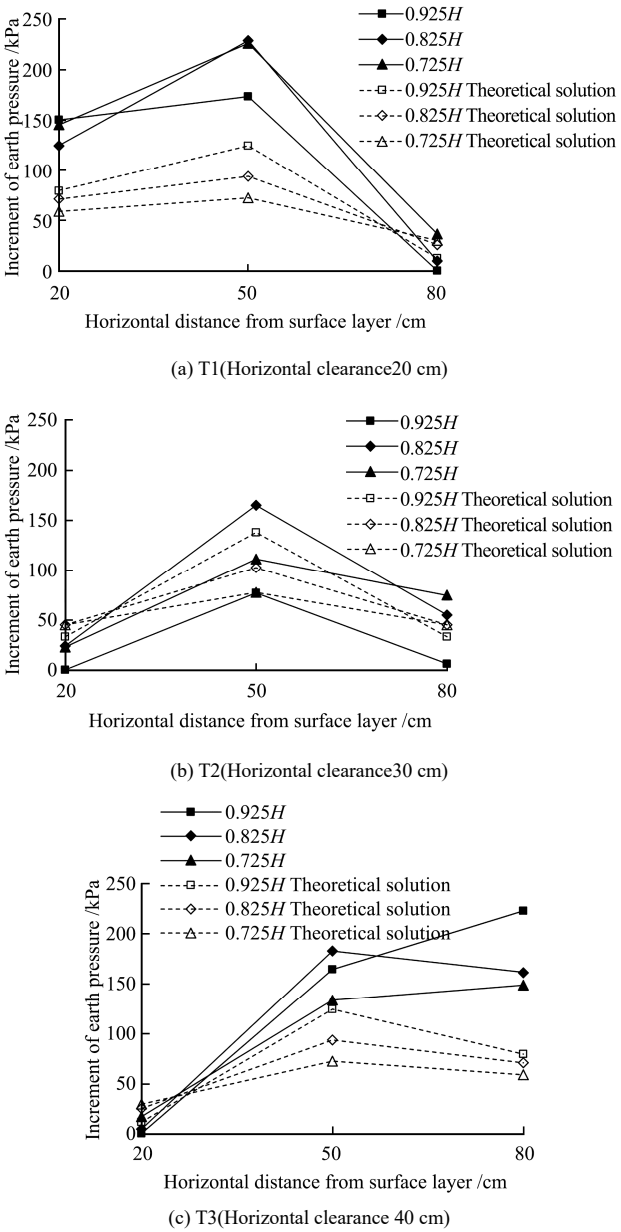

(a) T1(Horizontal clearance20 cm)

(b) T2(Horizontal clearance30 cm)

(c) T3(Horizontal clearance 40 cm)

Fig. 10 Distribution of vertical earth pressure under a 100 kN load

3.6 Strain of the reinforcement

For the sake of clarity, this paper only gives the results of measuring the strain of the reinforcement under the vertical load of level 3, as shown in Fig. 11. A few observations can be taken from the figure. ① The strain of the reinforcement increases with the increase of the additional load, and the maximum value of strain in each layer of the reinforcement is located under the load-bearing area, rather than the surface connection. ② As the horizontal clearance increases, the strain extremum of the reinforcement is also moving inward, getting farther and farther away from the surface layer. ③Considering the strain extremum of each layer of reinforcement, the extreme strain of the upper part of the abutment and near the load-bearing area is the largest, and it gradually decreases downward. To the lower part of the abutment, the extreme strain of the reinforcement is significantly reduced. This result reflects the deformation characteristics and working mechanism of the small-spacing reinforced soil abutment under vertical load, that is, the coordinated deformation of the reinforcement and the fill. In the area where the vertical stress is concentrated, the lateral deformation of the fill is large, and the strain of the reinforcement also increases simultaneously. The reinforcement exerts a lateral effect on the fill, instead of being subjected to lateral earth pressure as in conventional reinforced soil retaining walls, and then transmitted to the reinforcement.

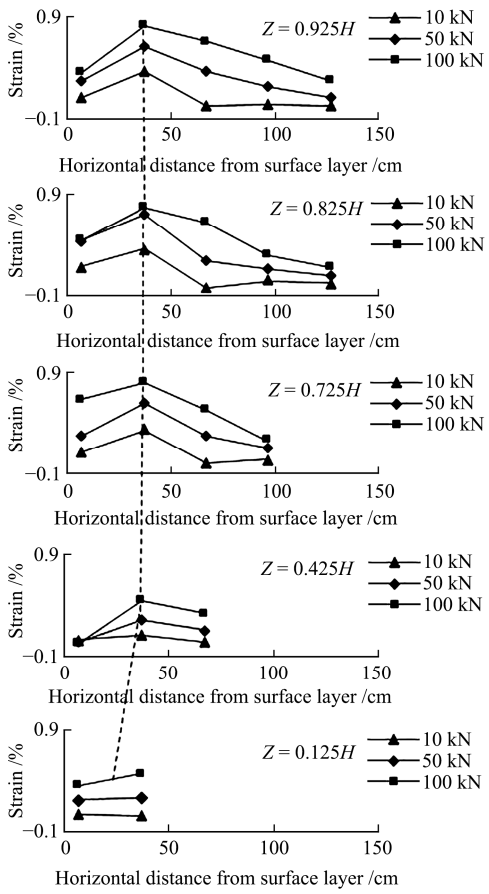

(a) T1 (Horizontal net distance 20 cm)

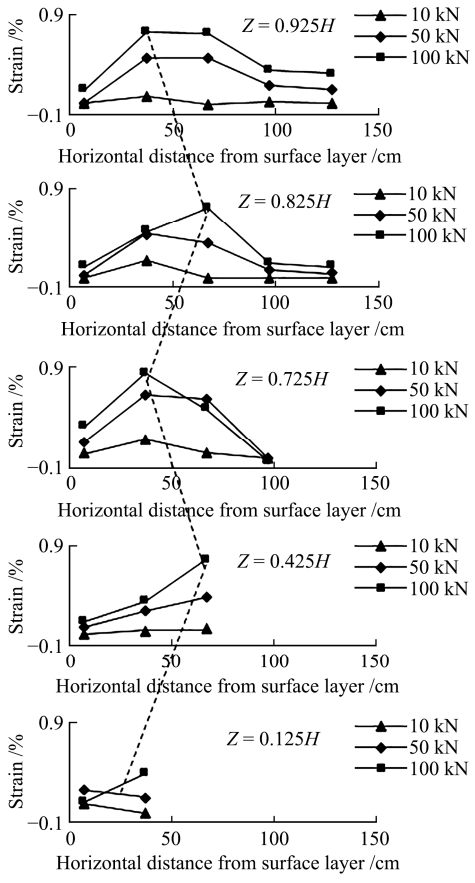

(b) T2 (Horizontal net distance 30 cm)

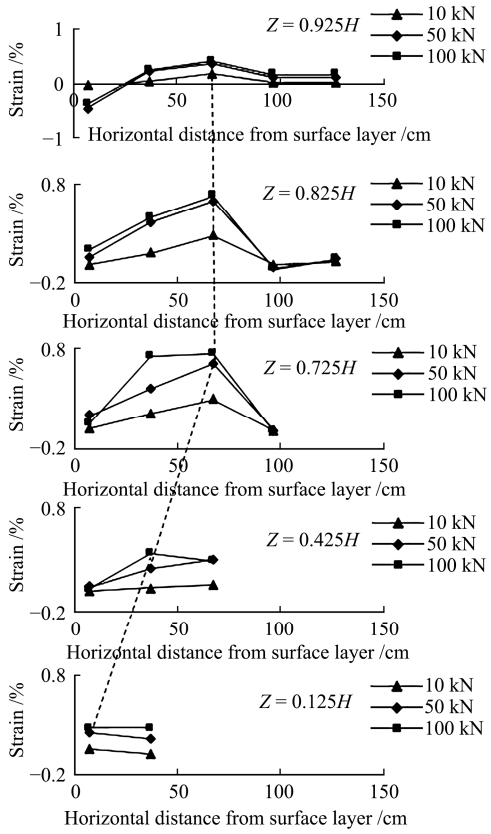

(c) T3 (Horizontal net distance 40 cm)

Fig. 11 Distribution of reinforcement strain along the length

The extreme value of the strain at the lower part of the reinforced soil abutment becomes smaller because the additional stress becomes smaller after spread and the bottom boundary also limits it.

If the extreme points of strain at each layer of reinforcement are connected (see Fig. 11) as the potential failure surface of the reinforced soil flexible abutment, the results of the three sets of model tests are not consistent. There seems to be no obvious regularity that can perfectly describe their correlation. Based on the test monitoring results, it can be inferred that the potential fracture surface is in the form of a double broken line. The lower part is close to the Rankine failure surface, while the upper part is a vertical surface related to the horizontal clearance and it passes through a certain position in the bearing area, rather than passing along the failure surface at the back of the bearing area. Similar results have been found by Gao et al.[16] and Wang et al.[17].

4 Conclusion

This paper presented the static load model test of the geotextile reinforced soil abutment. Through the analysis of the test results, the following conclusions can be drawn.

(1) With the gradual increase of the horizontal clearance,

the horizontal displacement of the abutment surface layer and the top settlement are decreasing and show convergence. The extreme value of strain of the reinforcement gradually decreases, indicating that within a certain range, increasing the horizontal clearance can increase the bearing capacity of the abutment, but an excessively large horizontal clearance is of little significance. When considering the actual bearing capacity of the reinforced abutment, the influence of the horizontal clearance should also be taken into consideration.

(2) The horizontal clearance has a significant effect on the distribution of the vertical additional stress in the abutment. When the horizontal clearance is 0.2H, the distribution of the vertical additional stress is roughly consistent with the theoretical solution of the corner point method, indicating that the abutment has good characteristics as a complex material.

(3) The test results show that the formula for calculating the ultimate bearing capacity of reinforced soil abutments in the current GRS-IBS design code in the United States may only be valid under specific fillers, reinforcements, and reinforcement methods. This design code needs to be further improved.

Due to the limitation of the test site conditions and the maximum loading capacity of the loading device, this test did not reach the ultimate bearing capacity of the reinforced soil abutment. The failure mode of the structure under the ultimate load state needs to be further investigated.

Reference

[1] ADAWS M T, SCHLATTER W, STABILE T. Geosynthetic reinforced soil integrated abutments at the Bowman Road Bridge in defiance county Ohio[C]//Geo-Denver. Reston: [s. n.], 2007.

[2] DAVID SUITS L. Geosynthetics, forging a path to bona fide engineering materials—a case study: geosynthetic reinforced soil–integrated bridge structure (GRS-IBS)[C]// American Society of Civil Engineers Geo-Chicago 2016. Chicago, Illinois: [s. n.], 2016.

[3] TALEBI MAJID, MEEHAN CHRISTOPHER L, LESHCHINSKY DOV. Applied bearing pressure beneath a reinforced soil foundation used in a geosynthetic reinforced soil integrated bridge system[J]. Geotextiles and Geomembranes, 2017, 45(6): 580−591.

[4] MOHAMED K, ABOUZAKHM M, ELIAS M. Applications and performance of geosynthetic-reinforced soil abutments on soft subsurface soil conditions[J]. Transportation Research Record: Journal of the Transportation Research Board, 2011, 2212(1): 74−81.

[5] MAMATHA K H, DINESH S V. Evaluation of strain modulus and deformation characteristics of geosynthetic-reinforced soil-aggregate system under repetitive loading[J]. International Journal of Geotechnical Engineering, 2018, 12(6): 545−555.

[6] HOFFMAN P, WU J T H. An analytical model for predicting load-deformation behavior of the FHWA GRS-IBS performance test[J]. International Journal of Geotechnical Engineering, 2015, 9(2): 150−162.

[7] NICKS J E, ESMAILI D, ADAMS M T. Deformations of geosynthetic reinforced soil under bridge service loads[J]. Geotextiles and Geomembranes, 2016, 44(4): 641−653.

[8] CAI Hua-nan. Experimental research on properties of strength and deformation of flexible reinforced soil composites[D]. Wuhan: Wuhan University of Technology, 2014.

[9] XU Chao, MEI Xue-song. Model test investigating the behavior of Geosynthetic-Reinforced soil(GRS) abutments subjected to static footing load[C]//Geosynthetics Conference. Houston: [s. n.], 2019.

[10] WHANG Chu-sheng, DU Hao-jie. Mechanical model test for determination of intervals of flexible abutment[J]. Mechanics in Engineering, 2004, 24(4): 33−36.

[11] WU J T H, PHAM T Q. Load-carrying capacity and required reinforcement strength of closely spaced soil-geosynthetic composites[J]. Journal of Geotechnical and Geo-environmental Engineering, 2013, 139(9): 1468−1476.

[12] XU C, LIANG C, SHEN P. Experimental and theoretical studies on the ultimate bearing capacity of geogrid-reinforced sand[J]. Geotextiles and Geomembranes, 2019, 47(3): 417−428.

[13] XIAO Cheng-zhi, LIU He, WANG Rong-xia, et al. Experimental study on performance of GRS bridge abutment with flexible face[J]. Chinese Journal of Geotechnical Engineering, 2013, 35(4): 169−174.

[14] MURAD ABU-FARSAKH, ALLAM ARDAH, GEORGE VOYIADJIS. 3D finite element analysis of the geosynthetic reinforced soil-integrated bridge system (GRS-IBS) under different loading conditions[J]. Transportation Geotechnics, 2018, 15: 70−83.

[15] ADAMS M, NICKS J. Design and construction guidelines for geosynthetic reinforced soil abutments and integrated bridge systems[R]//Design and Construction Guidelines for Geosynthetic Reinforced Soil Abutments and Integrated Bridge Systems. McLean: Federal Highway Administration, 2018.

[16] GAO Jiang-ping, YU Mao-hong, HU Chang-shun, et al. Large model experiment on sliding rupture of reinforced earth retaining wall[J]. Journal of Chang'an University (Natural Science Edition), 2005, 25(6): 6−9.

[17] WANG Jia-quan, XU Liang-jie, HUANG Shi-bin, et al. Bearing capacity analysis of geogrid reinforced abutment retaining wall under dynamic load[J]. Rock and Soil Mechanics, 2019, 40(11): 4220−4228.